

Directly driven Rayleigh–Taylor instability of modulated CH targets

Jia Guo(贾 果), Xiong Jun(熊 俊), Dong Jia-Qin(董佳钦)[†],
Xie Zhi-Yong(谢志勇), and Wu Jiang(吴 江)

Shanghai Institute of Laser Plasma, Shanghai 201800, China

(Received 21 June 2011; revised manuscript received 24 April 2012)

Directly driven ablative Rayleigh–Taylor (R–T) instability of modulated CH targets was studied using the face-on X-ray radiography on the Shen-Guang II device. We obtained temporal evolution images of the R–T instability perturbation. The R–T instability growth factor has been obtained by using the methods of fast Fourier transform and seeking difference of light intensity between the peak and the valley of the targets. Through comparing with the the theoretical simulation, we found that the experimental data had a good agreement with the theoretical simulation results before 1.8 ns, and was lower than the theoretical simulation results after that.

Keywords: Rayleigh–Taylor hydrodynamic instability, Fourier analysis, theoretical simulation

PACS: 52.57.–z, 02.30.Nw, 02.60.Cb

DOI: 10.1088/1674-1056/21/9/095202

1. Introduction

As is well known, the hydrodynamic interface instabilities, such as the Rayleigh–Taylor (R–T) instability, play an important role in inertial confinement fusion (ICF).^[1–4] In ICF implosions, initial perturbations on the target surface will grow primarily due to the R–T instability, resulting finally in fuel pusher mixing, which degrades the implosion performance. To limit the mixing within an acceptable level, profound understandings of the R–T instability are necessary. The R–T instability can be generally divided into linear-growth and nonlinear-growth regimes. The initial perturbation amplitude in most ICF targets is much smaller than that of the perturbation wave, so early in its development, the perturbation grows in the linear-growth regime with an exponential trend until the perturbation amplitude grows to 10% of that of the perturbation wave,^[5] then the R–T Instability comes into the nonlinear-growth regime, in which the perturbation amplitude grows slowly with a trend to saturate. So the perturbation growth in the linear-growth regime makes a major contribution to the R–T instability amplitude.^[6,7] The growth rate is expected to be an important physical parameter, which describes the growth of the R–T instability. But because of the nonuniformity of laser, the instability amplitude is hard to measure, and then is commonly ob-

tained by simulations. In practice, the growth factor is often used instead of the growth rate to describe the growth process of the R–T instability.

The experimental studies of the Rayleigh–Taylor instability mainly focus on two aspects, the sophisticated diagnostic technology and the targets. The former relies mainly on the optimization of diagnostic instruments and experimental conditions, including the progress of the imaging system and the development of different diagnostic types of targets.^[8] For example, the spherical bent crystal imaging technology can be used to obtain three-dimensional images, U.S. Naval Research Laboratory has done a series of experiments in this way.^[9–11] The use of VISAR (velocity interferometer system for any reflector) system to measure the spall development of the R–T instability provides a new way to carry out experimental studies.^[12,13] In the research of experimental contents, different kinds of experiments carried out depend on the the different stages of R–T instability growth. The linear-growth stage is the main stage of the R–T instability growth, and has been intensively studied. In ICF, the nonlinear-growth R–T instability may affect the mixing of hot spot materials, even leads to ignition failure. However, due to the limitations of diagnostic techniques, the numerical simulation is the main research tool used to study the nonlinear-growth stage and the turbulent stage.^[14,15] In this paper, we use

[†]Corresponding author. E-mail: dongjiaqin@hotmail.com

the single-mode modulation target to study the linear-growth stage of the R–T hydrodynamic instability.

The experiment was divided into two parts. Firstly, we obtained the R–T instability images of Al targets irradiated by 4.7 keV X-ray in 120 ps interval, which was recorded by CCD, this part of work has been reported in 2010.^[16] Secondly, we obtained the time-resolved image of CH targets irradiated by 1–2 keV X-ray in 2.4 ns. In this paper, we describe the second part of work.

2. Design of experiment and data processing results

The schematic view of the experimental setup is shown in Fig. 1. The targets were made of CH with a density of 1.02 g/cm³ and a thickness of 20 μm, the perturbation wavelength was designed into two periods, 27 μm and 75 μm, and the initial perturbation amplitude was about 1–2 μm. As for the drive beam, we used the ninth laser from the Shen-Guang II device smoothed by an LA plate, the trapezoidal wave, the energy was 800 J, the wavelength was 0.35 μm (frequency-tripled), the spot size was 800 μm×800 μm, and because of the optical arrangement, the ninth laser irradiated the CH targets at 45° in 2.2 ns. Four beams of the Shen-Guang II device irradiated at a Cu target to generate the 1–2 keV backlighting with the energy of 260 J/beam and the spot size of 500 μm in 2 ns, the full width at half maximum (FWHM) of the pulse was 2.4 ns measured with an oscilloscope. The temporal evolution image of the R–T instability of CH was obtained by using an X-ray streak camera with the face-on diagnostic method. We defined time zero ($t = 0$) as the time of half maximum of the ninth laser (main laser).

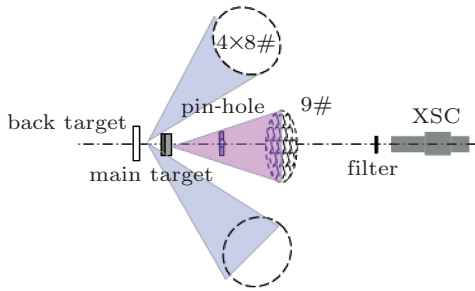


Fig. 1. (colour online) Schematic diagram of experimental setup.

Raw streaked images obtained in the face-on experiment are shown in Figs. 2(a) and 2(b). The spot

of the backlighting projected to the target is about 4–10 periods. The ninth laser is 0.49 ns earlier than the backlighting.

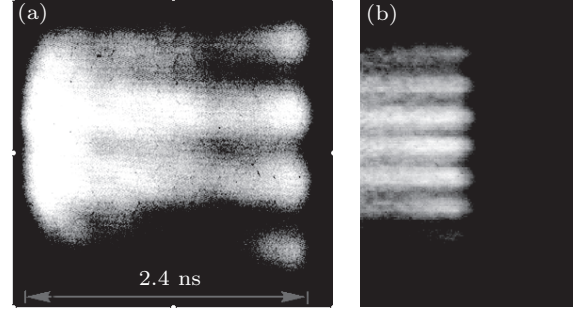


Fig. 2. Raw streaked images with the periods of (a) 75 μm and (b) 27 μm.

As is well known, the X-ray transmission formula is^[17]

$$I(t) = I_0 \exp^{-\mu \rho l t}, \quad (1)$$

where I_0 is the initial backlight intensity, μ is the mass absorption factor, and ρ is the density. So we can get $\sigma(t) = \mu \rho \eta = \ln(I_v(t)/I_p(t))$, where σ is the optical thickness, η is the amplitude of the modulated target, l_v is the backlight intensity at the valley of the target, and l_p is the backlight intensity at the peak of the target. To use the formula, we should assume that the backlight intensity is uniform. Using the obtained optical thickness, there are two ways to obtain the information of the R–T instability. First, if the density of the target over time can be measured, we can get the amplitude of the R–T instability over time. Second, through the fast Fourier transform (FFT) of the optical thickness, different harmonic modes of the R–T instability can be obtained.^[18] Because of the difficulty of measuring the density, we choose the second method to describe the growth of the R–T instability.

The backlight intensity distribution we used in experiment is similar to Gaussian, not the uniform distribution, and the experimental data are mixed with noise, so backlight fitting and smoothing data should be done first before using the intensity of the X-ray.^[10] The optical thickness versus time is shown in Fig. 3. The wavelength is 75 μm. The exponential fitting shows that the R–T instability is in the linear-growth regime. So we can have the following approximation:

$$\sigma = \mu \rho l = \mu \rho l_0 e^{\gamma t} \triangleq \mu \rho_0 l_0 e^{\tilde{\gamma} t} = \sigma_0 e^{\tilde{\gamma} t}. \quad (2)$$

For Fig. 2(a), we obtain $\sigma_0 \sim 0.0456 \pm 0.00317$, $\tilde{\gamma}_{75} \sim 0.81526 \pm 0.0276$, for Fig. 2(b), $\sigma_0 \sim 0.04818 \pm 0.01122$, $\tilde{\gamma}_{27} \sim 0.60869 \pm 0.10845$, σ_0 remains almost

unchanged, which shows that the approximation is effective. In experiment, the laser energy irradiated the 27 μm target (706 J) was lower than that irradiated the 75 μm target (829 J), so $\bar{\gamma}_{27} < \bar{\gamma}_{75}$ can be understood. Comparing with the work of Kilkenny *et al.*,^[18] we obtain a similar data fitting curve, which shows that the data we obtained are indeed in the linear-growth stage. But because our backlight time is shorter than their time (~ 5 ns), so we do not obtain the data of the latter growth in the linear-growth stage.

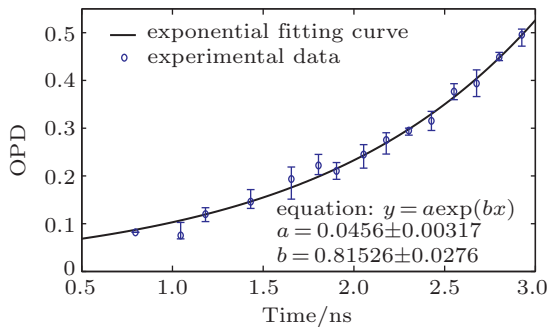


Fig. 3. (colour online) Optical thickness (OPD) with time.

In addition, with the development of the R-T instability, the perturbation on the interface grows more and more irregular, which means that higher harmonic modes will be obtained in the FFT of the optical thickness.

Figure 4 shows the different harmonic modes obtained in the FFT of the optical thickness of the 75 μm target. we find that the Fourier series are mainly distributed in the first to the third orders, and the values are small, so we can get the conclusion that in our experiment, the R-T instability is still in the linear-growth regime at 2.2 ns.

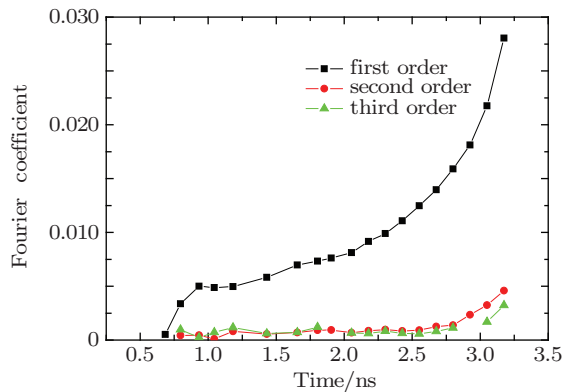


Fig. 4. (colour online) Fourier transform of the optical thickness

In the following, we will test whether our data processing is reasonable or not by comparing our processed experiment data with the simulation results (Fig. 5). In experiment, 0.8 ns after the main laser, the perturbation amplitude can be recorded clearly by the streak camera, so we choose the 0.8 ns after the main laser as the beginning of the data comparison.

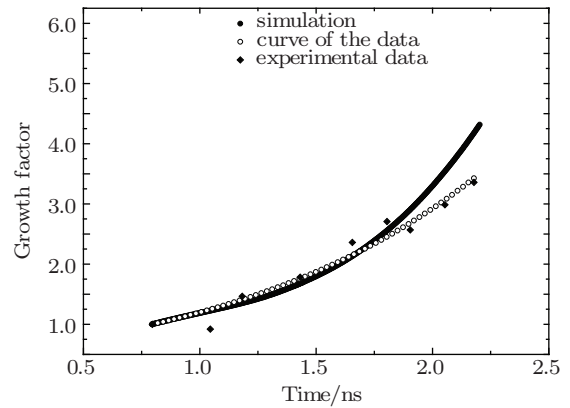


Fig. 5. Growth factor as a function of time for the 75 μm target.

In Fig. 5, before 1.8 ns, the processing data are in good agreement with the simulation results, between 1.8 ns and 2.3 ns, the experimental data are below the simulation results, and the minimum is 78% of the simulation result, so we consider that our data processing has a practical value.

3. Conclusion

In summary, we have shown the measurements of laser directly-driven Rayleigh–Taylor instability of modulated CH targets in the linear-growth regime. The optical thickness has been given by using the methods of FFT and seeking the difference between the peak and the valley of the image intensity. We also showed the different harmonic modes of the optical thickness, which illustrated that the R-T instability was still in the linear-growth regime. The experimental results were compared with the theoretical simulation, and a good agreement was obtained, this implies that our experimental data processing method has a practical value and can be applied to future Rayleigh–Taylor data processing.

Acknowledgement

We acknowledge the simulation supports given by Wu Jun-Feng and Ye Wen-Hua (Institute of Applied Physics and Computational Mathematics).

References

- [1] Chandrasekhar S 1968 *Hydrodynamic and Hydromagnetic Stability* (London: Oxford Univ. Press) Chap. 10
- [2] Nuckolls J, Wood L, Thiessen A and Zimmerman G 1972 *Nature* **239** 139
- [3] Shigeyama T and Nomoto K 1990 *Astrophys. J.* **360** 242
- [4] Arnett W 1989 *Astrophys. J.* **341** 63
- [5] Ye W H 1998 *High Power Laser and Particles Beams* **10** 4
- [6] Remington B A, Haan S W, Glendinning S G, Kilkenny J D, Munro D H and Wallance R J 1991 *Phys. Rev. Lett.* **67** 3259
- [7] Remington B A, Haan S W, Glendinning S G, Kilkenny J D, Munro D H and Wallance R J 1992 *Phys. Fluids B* **4** 967
- [8] Yang L B, Liao H D, Sun C W, Ou Y K M, Li J and Huang X B 2004 *Chin. Phys.* **13** 10
- [9] Pawley C J, Bondner S E, Dahlburg J P, Obenschain S P, Schmitt A J, Swthian J D and Sullivan C A 1999 *Phys. Plasmas* **6** 2
- [10] Menikoff R, Mjolsness R C, Sharp D H and Zemach C 1977 *Phys. Fluids* **20** 12
- [11] Bernstein B I and David L B 1983 *Phys. Fluids* **26** 453
- [12] Remington B A, Park H S, Lorenz K T, Cavallo R M, Pollaine S M, Prisbrey S T, Rudd R E, Becker R C and Bernier J V 2009 *Solid-state Rayleigh-Taylor Experiments in Vanadium at Mbar Pressures at the Omega Laser* LLNL-PROC-416238
- [13] Park H S, Lorenz K T, Cavallo R M, Pollaine SM, Prisbrey S T, Rudd R E, Becker R C, Bernier J V and Remington B A 2010 *Phys. Rev. Lett.* **104** 135504
- [14] Ye W H, Zhang W Y and Cheng G N 1998 *High Power Laser and Particle Beams* **10** 3
- [15] Piriz A R and López C J 2009 *Phys. Rev. E* **80** 046305
- [16] Jia G, Fu S Z, Dong J Q, Shu H, Xiong J and Gu Y 2010 *Chinese Journal of Lasers* **37** 1
- [17] Betti R, Goncharov V N, MacCrory R L and Verdon C P 1998 *Phys. Plasma* **5** 5
- [18] Kilkenny J D, Glendinning S G, Haan S W, Hammel B A, Lindl J D, Munro D, Remington B A, Weber S V, Knauer J P and Verdon C P 1994 *Phys. Plasmas* **1** 1379